European Journal of Pharmaceutics and Biopharmaceutics 134 (2019) 190–198

Contents lists available at ScienceDirect

European Journal of Pharmaceutics and Biopharmaceutics

journal homepage: www.elsevier.com/locate/ejpb

Research paper

Sortagging of liposomes with a murine CD11b-specific VHH increases in vitro and in vivo targeting specificity of myeloid cells

Steffen Wöll[a,c,*], Christopher Bachran[b], Stefan Schiller[a], Matthias Schröder[b], Lena Conrad[b], Regina Scherließ[c], Lee Kim Swee[b]

[a] Merck KGaA, Frankfurter Str. 250, 64293 Darmstadt, Germany
[b] BioMed X GmbH, Im Neuenheimer Feld 583, 69120 Heidelberg, Germany
[c] Department of Pharmaceutics and Biopharmaceutics, Kiel University, Grasweg 9a, 24118 Kiel, Germany

ARTICLE INFO

Keywords:
Immunoliposomes
Targeted drug delivery
Sortase-A
Liposome purification
Myeloid derived suppressor cells
CD11b
Gr-1

ABSTRACT

The therapeutic index of drugs can be increased via drug encapsulation in actively targeted, meaning ligand modified drug delivery systems. The manufacturing of such targeted drug delivery systems, in particular the conjugation between drug carrier and ligand, can be done by enzymatic conjugation methods, exploiting the site-specific, bioorthogonal nature of these reactions. The use of such enzymes like Sortase-A transpeptidase requires efficient purification methods, as residuals of the enzyme may be responsible for immunogenic potential and drug product instabilities. These instabilities may be based on the enzymatic reverse reaction, meaning here a cleavage between ligand and drug carrier. In the presented work, two differently PEGylated formulations were modified with variable fragments of camelid heavy chain-only antibodies (VHH) via Sortase-A, purified by different methodologies and tested for ligand cleavage upon storage. Strongly PEGylated liposomes (PEG^{high}-LS) were found to retain higher amounts of Sortase-A than lowly PEGylated ones (PEG^{low}-LS) after dialysis purification. Surprisingly, this did not correlate with ligand stability during storage. PEG^{high}-LS were less prone for degradation, compared to PEG^{low}-LS, which showed a ligand cleavage of 20% after an 8 weeks storage at 2–8 °C. Nonetheless, overall degradation could be minimized by an additional affinity bead purification procedure. Liposomes modified with a CD11b-specific VHH were tested for their in vitro and in vivo targeting ability towards $CD11b^+$ cells. Specific targeting of CD11b was achieved in vitro and in vivo on various cell types. PEGylation decreased the targeting effect in vitro, however no differences between PEG^{high} or PEG^{low} formulations were observed in vivo. The obtained results underline the need for a thorough characterization of novel conjugation strategies as well as an early in vivo characterization of such targeted drug delivery systems.

1. Introduction

The use of enzyme-mediated transpeptidation techniques has proven valuable for protein modifications in many examples. These include payload [1] or fluorophore conjugation [2] for antibody-drug conjugates and diagnostics, the lipidation [3] and glycosylation [4] of proteins and decoration of drug delivery systems with targeting ligands [5–9]. Amongst other enzymes such as transglutaminase [10] and butelase [11], Sortase-A is the most widely used enzyme for such applications [12,13]. The main advantages of Sortase-catalyzed reactions are the inherent site-specificity, mild conjugation conditions and short recognition motifs in substrate proteins [12,13]. Sortase variants have been extensively studied regarding structure [14], substrate specificity [9], reaction kinetics [15] and conditions [12]. Sortase-A recognizes a C-terminal amino acid sequence of LPxTG (leucine-proline-any amino acid-threonine-glycine) and forms a thioester as intermediate between threonine and glycine. Subsequently, a nucleophile, typically an oligoglycine, forms a peptide bond between threonine's carboxylic acid group and the oligoglycine's free amine [12,13]. A major drawback of Sortase-A reaction is the reversibility of the transpeptidation [11]. The reverse reaction can be defined as the formation of the thioester intermediate of a newly formed LPxTG motif, followed by a nucleophilic attack of (a) the previously cleaved sequence from the substrate with the N-terminal glycine, (b) the desired glycine-nucleophile again leading to the reaction product, or (c) a water molecule [16,17]. Latter causes hydrolysis of the LPxTG motif and loss of recognition for the transpeptidation reaction. This reverse reaction can therefore decrease overall conversion rates [7,11]. Furthermore, although Sortase-A

* Corresponding author at: Merck KGaA, Frankfurter Str. 250, 64293 Darmstadt, Germany.
E-mail address: steffen.woell@merckgroup.com (S. Wöll).

https://doi.org/10.1016/j.ejpb.2018.11.014
Received 24 September 2018; Received in revised form 15 November 2018; Accepted 16 November 2018
Available online 20 November 2018
0939-6411/

reaction is considered as site-specific and reaction products should be homogeneous, structural variants of the product are obtained by reverse reactions especially if substrates carry several LPxTG motifs. This is typically the case in the synthesis of antibody-drug conjugates [1], where equilibrium processes between payload conjugation and hydrolysis may lead to different drug-to-antibody ratio species. Reversibility of the reaction further necessitates high demands on product purification. Besides the immunogenic potential of Sortase-A residuals in drug product formulations, traces of the enzyme may be responsible for a drug product instability, manifested in the subsequent hydrolysis of the LPxTG motif between the conjugated substrates. This would, in case of antibody-drug conjugates, lead to an increase of the free drug, or in case of drug delivery systems, cleavage of the targeting ligand from the particulate construct. A robust and efficient purification from Sortase-A is therefore of utmost importance for the use of this technology.

We recently demonstrated high dependency of liposomal surface properties on the transpeptidation reactivity of pentaglycine – liposomes towards LPETG modified single-domain antibodies of camelid heavy chain only antibodies (VHHs) [18]. PEG-shielding of a pentaglycine moiety on the bilayer surface led to a drastically decreased conversion rate. Furthermore, reaction kinetics indicated influence of the PEGylation status on the extend of the reverse reaction during the ligand conjugation. Besides this, we observed retention of Sortase-A over dialysis purification, which occurred preferentially for 2 kDa PEG-derivatized liposomes. We therefore investigated here the stability of the VHH bound to the liposomal system to analyze if purification methods or liposomal surface properties influence hydrolysis stability of the targeting ligand upon storage.

In vitro targeting of $CD11b^+$ human myeloid cells via a CD11b-specific VHH modified liposomal system was recently achieved with high specificity [18]. To further demonstrate the feasibility to target desired cell types in vivo with sortaggable liposomes, a VHH (VHH DC13) which binds murine myeloid cell surface receptor CD11b [2,19] was employed as targeting ligand. CD11b is an integrin expressed on various myeloid cells such as monocytes, granulocytes, dendritic cells, macrophages and myeloid derived suppressor cells (MDSC). MDSC are a heterogeneous cell population expanding under pathologic conditions such as cancer, trauma or sepsis that can inhibit the function of effector T cells [20]. Specific delivery of cargos such as antigens or toxins to myeloid cells can be used for therapeutic purposes as vaccines to increase adaptive immune response (antigen cargo) or to deplete cells (toxin cargo) that contribute to cancer progression (e.g. MDSC). Recently, VHHs against myeloid cell surface markers Gr-1 and CD11b were conjugated to the catalytic domains of *Pseudomonas* exotoxin A, a potent bacterial toxin. The immunotoxins were able to deplete mono- or granulocytes in vivo with a target-, cell- and organ-dependent activity [19]. In the present work, we investigated whether the described sortaggable liposomal drug delivery systems could be decorated with VHH DC13 by Sortase-A and directed towards murine $CD11b^+$ $Gr\text{-}1^+$ myeloid cells. For that purpose, binding of fluorescence-labeled liposomes was tested in vitro with different immune cell lines and primary splenocytes. Furthermore, specificity of targeting myeloid cells was investigated in vivo and analyzed with flow cytometry by staining murine splenocytes for myeloid ($Gr\text{-}1^+/CD11b^+$) or lymphoid ($CD3^+$ or $CD19^+$) subpopulations. With the present work, we analyzed for the first time the active in vivo targeting of $CD11b^+$ myeloid cells via a liposomal system. Our results demonstrate feasibility for a cell-selective drug delivery towards these immune cells and can be useful for novel therapeutic approaches in immuno-oncology.

2. Materials

Glycine modified lipid DMA-PEG-G5 was obtained from Merck & Cie, Schaffhausen, Switzerland and is described in detail elsewhere [21]. In brief, the lipid consists of a pentaglycine structure conjugated to a 2 kDa monodisperse PEG-spacer, followed by a bilayer anchor (dimyristyl-amino-propandiol; DMA). 1,2-dipalmitoyl-*sn*-glycero-3-phosphocholine (DPPC), 1,2-dipalmitoyl-*sn*-glycero-3-phospho-(1′-*rac*-glycerol) (DPPG) and 1,2-distearoyl-*sn*-glycero-3-phosphoethanolamine-N-[methoxy(polyethylene glycol)-2000] (DSPE-mPEG) were a gift of Lipoid GmbH, Ludwigshafen, Germany. DPBS (Dulbecco's phosphate buffered saline, D1408, 10fold stock), FITC-dextran 10 kDa and cholesterol were purchased from MilliporeSigma (St. Louis, Missouri, USA). Acetonitrile, trifluoroacetic acid (TFA), methanol and ethanol (both gradient grade) were obtained from Merck KGaA, Darmstadt, Germany. MilliQ water was taken from a Millipore Advantage A 10 with Q-Pod apparatus (Merck KGaA, Darmstadt, Germany). Sortase-A, VHH ENH and VHH DC13 were prepared as described in [19].

3. Methods

3.1. Liposome preparation

Pentaglycine modified liposomes were prepared by a solvent injection process described in detail elsewhere [18]. Liposomes consisted of 1 mol% DMA-PEG-G5, DPPC (59.4 mol%), cholesterol (34.7 mol%) and 5.0 mol% of either DSPE-mPEG (referred to as "PEG^{high}-LS") or DPPG (referred to as "PEG^{low}-LS"). In brief, the lipids were dissolved to 90 mM in ethanol (PEG^{high}-LS) or to 32 mM in methanol (PEG^{low}-LS). The lipid solutions were injected by a syringe pump (PHD Ultra4400, Harvard Apparatus, Holliston, Massachusetts, USA) into a stream of DPBS pH 7.4 conveyed by a peristaltic pump (Ismatec IP65, Cole-Parmer, Wertheim, Germany). Lipid and buffer streams were connected via a stainless steel, luer-lock T-piece (Unimed S.A., Lausanne, Switzerland), customized with a 27 G needle for lipid injection. 10 mg/mL FITC-dextran was added to the injection buffer for the manufacturing of FITC labeled liposomes. Dispersions obtained from injection were purified and concentrated by tangential flow filtration [21].

3.2. Ligand conjugation and purification

For analysis of purification dependent ligand stability, PEG^{high}-LS and PEG^{low}-LS were conjugated to the model single-domain antibody VHH ENH [22]. Liposomes (100 μM total pentaglycine), VHH ENH (50 μM) and 25 μM of Ca^{2+}-independent, 6-histidin (his) tagged Sortase-A variant SortA7m were incubated for 4 h at 4 °C. An aliquot of the reaction mixture was retained for further analysis, remaining liposomes were dialyzed (Float-A-Lyzer, MWCO 1000 kDa, G235037, Spectrum Labs, Los Angeles, California, USA) against 100-200fold acceptor medium (DPBS) with five buffer changes over 24 h. A further aliquot was additionally refined with his-tag binding magnetic sepharose-nickel beads (GE Healthcare, Chaltfont St Giles, UK) to remove residual amounts of Sortase-A or VHH. For that, 100 μL bead slurry was washed three times with DPBS using a magnetic rack. Supernatant was removed, and the beads were redispersed with 200 μL of the liposomal dispersion. After 2 h incubation at 4 °C and gentle shaking, magnetic beads were removed. Non-purified, dialyzed and additional bead purified liposomes were stored in Teflon-sealed glass vials for analysis of physical liposome stability (hydrodynamic diameter, polydispersity index, zeta potential) and chemical stability of the targeting ligand. For in vitro and in vivo experiments, FITC labeled liposomes were either modified with VHH ENH (isotype control) or murine CD11b binding VHH DC13, followed by dialysis purification.

3.3. Liposome characterization

Liposomes were analyzed for hydrodynamic diameter d_h and polydispersity index (PDI) using a DynaPro Plate Reader II, Wyatt Technology Corporation, Santa Barbara, California, USA. Zeta potential was measured after dilution to 3% v/v in 10 mM NaCl using a Malvern Zetasizer Nano ZS, Worcestershire, UK. Detailed measurement settings are described elsewhere [18]. Molecular bilayer compositions were

determined by an rp-HPLC method (based on a C18-column) with evaporative light scattering as described earlier [21].

For quantification of conjugated VHH on the liposomes, a second rp-HPLC method (based on a C4 column), which separates proteins, DMA-PEG-G5 modified VHHs and lipid components of the liposome from each other was used [18]. For that, non-liposomal conjugates were synthesized, isolated by rp-HPLC and redispersed in water. Concentration was determined by UV-spectroscopy (NP80, Implen, Westlake Village, California, USA) using calculated extinction coefficients (ExPASy ProtParam, SIB, Lausanne, Switzerland). Isolated conjugates were used as HPLC-reference standard at 280 nm to determine concentration of VHH-lipid conjugates on liposomes after injection of 5 µL liposomal dispersion. VHH-conjugate content was normalized on phospholipid content, and the reaction efficacy was calculated (Eq. (1), t_i: after sortagging and purification; t_0: start of the reaction).

Equation (1)

$$reaction\ \ efficacy\ \ [\%] = \frac{\frac{c_{VHH-conjugate}}{c_{lipid}}(t_i)}{\frac{c_{VHH}}{c_{lipid}}(t_0)} * 100 \quad (1)$$

Furthermore, residual amounts of Sortase-A after dialysis or bead purification were determined by rp-HPLC based on a 25 µM Sortase-A reference measured at 280 nm. Limit of quantification (LOQ) of this method was 3.1 µM for a signal to noise ratio of 10:1 as determined by the chromatography software (OpenLab CDS EZChrom, Agilent Technologies).

To investigate stability of the targeting ligand regarding hydrolytic cleavage, liposomal samples were stored at 2–8 °C for 8 weeks and analyzed by rp-HPLC for change in the relative area of the lipidated VHH. Stability was calculated according to Eq. (2), where t_i is the actual pull point and t_0 the start value of the study. Results of three batches were averaged.

Equation (2)

$$stability\ \ S_{rel} = \frac{area\%_{VHH-conjugate}(t_i)}{area\%_{VHH-conjugate}(t_0)} \quad (2)$$

Total FITC content of dye-labeled batches was determined by fluorimetry (M200 plate reader, Tecan Group, Männedorf, Switzerland) after a lysis of the liposomes in Triton-X 100. Free FITC-dextran was determined by analytical size exclusion chromatography described in [18] with fluorescence detection (excitation: zero order, emission: 510 nm) separating liposomes and non-encapsulated FITC-dextran. Encapsulated FITC-dextran was calculated as total – free FITC-dextran. Encapsulation efficiency was calculated as the ratio of FITC-dextran per lipid of the final dispersion, divided by the theoretical ratio of FITC-dextran per lipid after solvent injection.

3.4. In vitro characterization of VHH DC13-liposomes

In cell culture DC2.4 cells and RAW macrophages were maintained in DMEM (Life Technologies, #61965026) supplemented with 10% heat-inactivated fetal bovine serum (FBS, Life Technologies, #10270106), 100 U/mL penicillin (Life Technologies, #15140122), and 100 µg/mL streptomycin (Life Technologies, #15140122). NUP progenitor cells (hematopoietic progenitors immortalized using a NUP98/HOXB4 transgene, described in [23]) and NUP-derived myeloid-derived suppressor cells (MDSC) were cultured in complete RPMI consisting of RPMI 1640 medium (Life Technologies, #21875-034) supplemented with 10% FBS, 100 U/mL penicillin, 100 µg/mL streptomycin, 1 mM sodium pyruvate (Life Technologies, #11360070), 50 µM 2-mercaptoethanol (Life Technologies, #31350-010) and 1 × non-essential amino acids (Life Technologies, #11140-035). MDSC were differentiated from NUP cells by 4 days of incubation in the presence of 20 ng/mL IL-6 (Biolegend, #570802) and 20 ng/mL murine GM-CSF (Biolegend, #576304) [24]. Splenocytes were isolated from a C57BL6/J mouse by mashing the spleen in a 70 µm cell strainer (Corning, #352350) and washing cells in FACS buffer (1 × PBS (Life Technologies, #14190-094) with 2% FBS). Cells were resuspended in 1 mL ACK (ammonium-chloride-potassium) lysing buffer (Thermo Fisher Scientific, #A10492-01) to remove red cells, incubated 5 min at room temperature, followed by addition of 5 mL FACS buffer and re-centrifuged.

For binding experiments 1×10^5 DC2.4 cells or RAW macrophages were seeded in a 96-well plate in 200 µL medium and kept overnight at 37 °C in the presence of 5% CO_2 before addition of liposomes. 2×10^5 NUP cells, MDSC or splenocytes were seeded in a 96-well plate in 200 µL. 100 µM of PEG^{high}-LS or PEG^{low}-LS (based on total lipid content of FITC labeled formulation, either as ligand free control (G5-LS), VHH ENH-decorated or VHH DC13-decorated liposomes) in 200 µL complete RPMI medium were added to each sample in V-bottom-shaped 96-well plates and incubated at 37 °C for 4 h in the presence of 5% CO_2. Afterwards, cells were centrifugated (300*g* for 1 min). The supernatant containing unbound liposomes was removed, followed by redispersion of the cells in FACS buffer by multiple pipetting cycles. Antibody staining of cells was performed in presence of Fc receptor block (TruStain fcX BioLegend, #422302) in FACS buffer. SytoxBlue (Thermo Fisher Scientific, S34857) was used for exclusion of dead cells. Following antibodies from BioLegend were used for flow cytometry: Brilliant Violet 605-anti-Gr-1 (#108439), PerCP-anti-CD11b (#101229), BV605-anti-CD3 (#100237) and APC-anti-CD19 (#115511).

For confocal microscopy, 0.5×10^6 RAW macrophages were seeded in a total volume of 200 µL complete RPMI. 100 µM liposomes were added to each sample in V-bottom-shaped 96-well plates and incubated at 37 °C for 4 h in the presence of 5% CO_2. Cells were stained with CellMask Deep Red Plasma membrane stain (1:5000) (Life Technologies, #C10046) and Hoechst 33342 (1:2000) (Thermo Scientific, #62249) for 15 min at 37 °C in the presence of 5% CO_2. The medium was removed by centrifugation (1 min at 300*g*), cells were washed with FACS buffer, transferred in 100 µL FACS buffer on poly-ethyleneimine-coated cover slips (microscope cover glasses from Marienfeld, 18 mm diameter, #0117580) and incubated for 10 min at 37 °C. Cells were fixed on cover slips with paraformaldehyde (final concentration 4%) for 15 min and washed with 1 × PBS. Cover slips were mounted on cover glass (neoLab, #1-6273) using anti-fade ProLong Diamond mounting medium (Invitrogen, #P36961) and analyzed 18 h later with a Leica TCS SP5 confocal microscope using an HCX Plan APO 40×/1.30 Oil CS objective. For image analysis the Leica Application Suite software was used.

3.5. In vivo targeting of MDSC

C57BL/6J mice were maintained under specific pathogen–free conditions in the animal facility of the University of Heidelberg. All animal experiments were done in accordance with German legislation governing animal studies (approved project G-250/14 by the Regierungspräsidium Karlsruhe). Female C57BL/6J mice (8 weeks old, Charles River) were injected intravenously with PBS (one animal) or 0.6 mM (based on total lipid content) of either VHH ENH-PEG^{low}-LS, VHH DC13-PEG^{high}-LS or VHH DC13-PEG^{low}-LS in 200 µL PBS (each 3 animals per group). After 2 h mice were sacrificed and splenocytes were isolated as described above. Splenocytes were stained for flow cytometry analysis using the same antibodies as described above. Statistically significant differences ($p < 0.05$) of FACS measurements were determined by unpaired *t*-test (Graph Pad Prism 7.03).

Table 1
Physico-chemical properties of unmodified and VHH-modified PEG^{high}-LS and PEG^{low}-LS (data shown as mean ± standard deviation of three reactions from one liposome bulk).

Formulation	d_h [nm]	PDI	Zeta potential [mV]
PEG^{high}-LS			
PEG^{high}-LS (unmodified)	140	0.22	−9.3
VHH ENH-PEG^{high}-LS (dialysis)	141 ± 1	0.22 ± 0.01	−5.7 ± 0.3
VHH ENH-PEG^{high}-LS (bead)	143 ± 0	0.22 ± 0.02	−6.1 ± 0.1
PEG^{low}-LS			
PEG^{low}-LS (unmodified)	175	0.23	−25.8
VHH ENH-PEG^{low}-LS (dialysis)	186 ± 4	0.23 ± 0.01	−17.3 ± 0.8
VHH ENH-PEG^{low}-LS (bead)	187 ± 2	0.23 ± 0.01	−17.2 ± 0.7

4. Results and discussion

4.1. VHH conjugation, purification and stability of the immunoliposomes

To investigate the formulation- and purification-dependent stability of liposomes conjugated with VHHs via Sortase-A, two sortaggable liposome types differing in the bilayer surface properties were prepared by solvent injection. Physicochemical parameters are described in Table 1. Sortase-A was used to ligate a LPETG-modified VHH (VHH "enhancer", described in [22]) towards the liposomes, followed by a dialysis step to remove the enzyme and unbound VHH. The sortagging and dialysis process had no relevant influence on size or PDI (Fig. 1A) as relative changes were below 10%. Zeta potential showed a shift towards neutral values with relative changes > 30%, however absolute changes were small (Table 1).

We previously observed a formulation dependent retention of Sortase-A after a dialysis purification step [18]. This encouraged us here to add an additional magnetic bead purification step [19] after the dialysis protocol to enhance removal of free Sortase-A from the liposomal dispersion. Here, his-tagged Sortase-A is bound towards Ni^{2+}-chelate beads. As the use of such magnetic bead systems for purification of liposomes was previously not described, we investigated compatibility regarding physical (size, PDI and zeta potential) and chemical properties (bilayer composition and VHH-density) of the liposomes. Neither size, PDI nor zeta potential showed relevant changes during the incubation process, indicating no alteration of the particle size distribution or surface properties by shear forces or other impacts through the beads (Fig. 1; Table 1). Furthermore, we investigated the influence of the sortagging and purification processes on the bilayer composition of the liposomes. The bilayer fraction of the reaction educt DMA-PEG-G5 showed a clear decrease after sortagging, showing the consumption of this lipid by the transpeptidation reaction. No other major changes occurred, indicating no adsorption to the dialysis membrane or device housing. Absolute lipid yields from dialysis devices were > 88% for PEG^{high}-LS and > 97% for PEG^{low}-LS. Bead purification was compatible with both liposomal compositions as the bilayer compositions were maintained (Table 2). This and the high overall lipid yields (> 90% for both formulation types, Table 2) indicated no adsorption of lipids to the sepharose bead material.

Residual Sortase-A levels were analyzed after dialysis and bead purification. PEG^{high}-LS retained high amounts of Sortase-A after dialysis (Fig. 2; Table 3). This is a surprising result as the cut-off of the dialysis device was ≈ 50fold larger than the molecular weight of this Sortase-A variant (20.9 kDa).

It is expected that an unspecific binding towards the PEG^{high}-LS may have occurred. The DPPG-stabilized formulation did hardly retain any non-lipidated protein over the dialysis process. A reason for the lower adsorption tendency of Sortase-A to the DPPG stabilized bilayers may be the significantly lower zeta potential. This may lead to a higher repulsion between Sortase-A and liposome surface, and finally a more effective dialysis purification. It was tested whether an additional affinity-based bead purification could further reduce Sortase-A residuals in the liposomal formulations. Though the Ni^{2+}-chelate beads should bind and therefore be able to remove the his-tagged enzyme, Sortase-A content in PEG^{high}-LS formulation was reduced only to a minor extend (Table 3).

This indicates a strong interaction with the liposomal surface, and may be origin of product instabilities, meaning a cleavage of the targeting ligand from the liposomal system via the reverse reaction of Sortase-A. Stability of the differently purified liposomal dispersions were therefore analyzed for cleavage of the targeting ligand upon storage at 2–8 °C. Non-purified feedstock from conjugation bulk of both formulations showed a pronounced loss of targeting ligand over storage (Fig. 3). Degradation rates were significantly higher for PEG^{low}-LS compared to PEG^{high}-LS. This is in congruence with results obtained earlier for the monitoring of the reaction kinetics on these two formulations, which showed a predominant reverse reaction for PEG^{low}-LS already after 14 h [18]. Most surprisingly, extend of targeting cleavage was independent of residual Sortase-A content. Although PEG^{high}-LS contained significant amounts of Sortase-A after both dialysis and bead purification steps, hardly any cleavage of the lipidated VHH was observed over the stability study (Fig. 3). In contrast to that, dialyzed PEG^{low}-LS showed a decrease of the VHH conjugated to the liposomes over 8 weeks (Fig. 3B; triangles). Assuming a homogenous loss of ligand over the liposomal dispersion, the average ligand density on a single

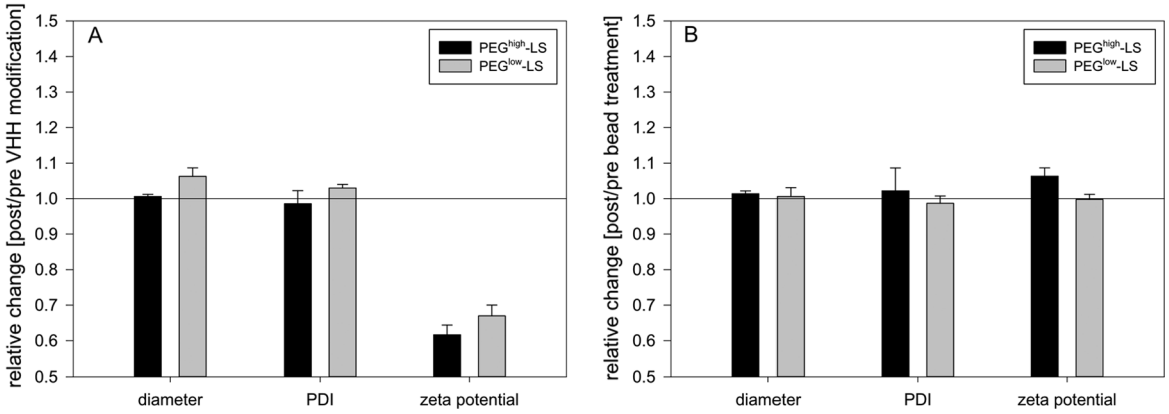

Fig. 1. Physico-chemical impact of VHH conjugation (A) and bead purification (B) on PEG^{high}-LS and PEG^{low}-LS. **A**: Minor affection of hydrodynamic diameter and PDI indicates colloidal stability of the nanoparticulate dispersion during ligand modification. Zeta potential showed low absolute, but clear relative changes due to surface modification and thereby charge alteration. **B**: His-tag affinity based magnetic bead purification does not affect integrity of targeted liposomal formulations as neither d_h, PDI nor zeta potential showed relevant changes. Data shown as mean ± standard deviation of three reactions and purifications from one liposome bulk.

Table 2
Molecular composition and purification yield of VHH ENH modified formulations (data shown as mean ± standard deviation of three reactions and purification procedures).

	DMA-PEG-G5 [mol%]	CHOL [mol%]	DPPC [mol%]	DPPG/DSPE-mPEG [mol%]	yield [%]
PEG^{high}-LS					
PEG^{high}-LS (unmodified)	1.0	35.2	59.4	4.5	
VHH ENH-PEG^{high}-LS (dialysis)	0.6 ± 0.0	34.8 ± 0.3	60.4 ± 0.2	4.2 ± 0.1	88.1 ± 1.4
VHH ENH-PEG^{high}-LS (bead)	0.6 ± 0.0	35.0 ± 0.6	60.5 ± 0.6	3.8 ± 0.1	90.4 ± 4.0
PEG^{low}-LS					
PEG^{low}-LS (unmodified)	1.0	35.2	59.50	4.3	
VHH ENH-PEG^{low}-LS (dialysis)	0.7 ± 0.0	34.3 ± 0.6	60.9 ± 0.9	4.2 ± 0.4	97.2 ± 2.5
VHH ENH-PEG^{low}-LS (bead)	0.7 ± 0.0	34.9 ± 0.4	60.1 ± 0.3	4.4 ± 0.1	96.8 ± 3.6

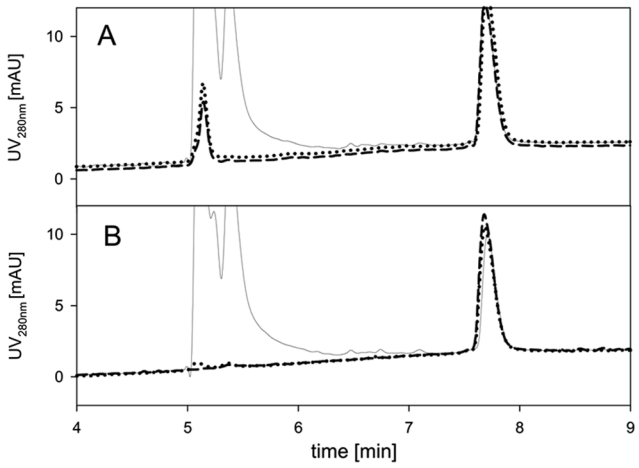

Fig. 2. Purification of PEG^{high}-LS (A) and PEG^{low}-LS (B) by dialysis (dotted) and magnetic beads (dashed). Solid chromatogram indicates unpurified reaction bulk. Peak at 5.0–5.3 min: Sortase-A; peak at 5.3–6 min: unbound VHH; peak at 7.8 min: lipidated VHH.

Table 3
Purification and VHH conjugation efficacy. Residual Sortase-A levels were below limit of quantification (LOQ) for the PEG^{low}-LS. PEG^{high}-LS retained considerable amounts of the enzyme over dialysis and the additional bead purification procedure. Data shown as mean ± standard deviation of three reactions and purification procedures.

Formulation	Residual Sortase-A [μM]	Reaction efficacy [%]
VHH ENH-PEG^{high}-LS (dialysis)	6.0 ± 0.6	33 ± 2
VHH ENH-PEG^{high}-LS (bead)	4.8 ± 0.6	34 ± 1
VHH ENH-PEG^{low}-LS (dialysis)	< 3.1 (LOQ)	28 ± 1
VHH ENH-PEG^{low}-LS (bead)	< 3.1 (LOQ)	28 ± 4

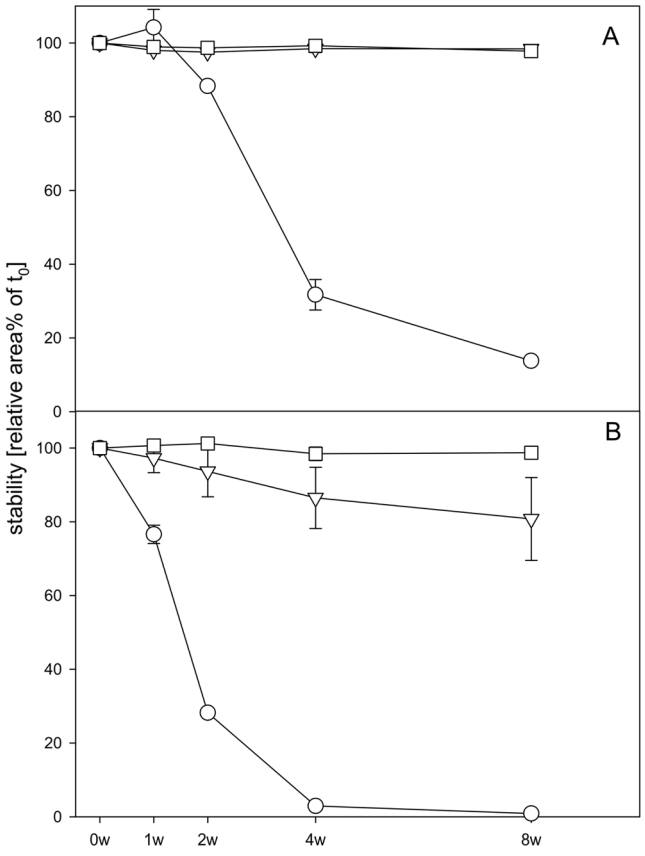

Fig. 3. Stability of VHH conjugated to the liposomes. Extent of targeting ligand cleavage by Sortase-A during storage is dependent on the PEGylation status. **A**: PEG^{high}-LS; **B**: PEG^{low}-LS. Circles: unpurified feedstock containing Sortase-A; triangles: dialyzed feedstock; squares: dialyzed and bead purified feedstock. Data shown as mean ± standard deviation of three reactions and purification procedures.

liposome decreased about 20% during storage. As latter is a critical value for an effective targeting [25], such a decrease would be inacceptable for a commercial product. Though not correlated in a quantitative manner with residual Sortase-A levels due to the quantification limit of the rp-HPLC method, this instability was overcome by the additional bead purification, as the bead purified PEG^{low}-LS did not show degradation over the study time.

It is suggested that a further reduction of the Sortase-A residuals by a his-tag mediated removal through the Ni^{2+}-chelate beads increased overall storage stability. It remains unclear why PEG^{low}-LS are more prone to the reverse reaction and hence lability during storage. Comparing surface properties of both formulations, PEG^{high}-LS contain an additional 2 kDa PEG-layer, that may protect the newly formed LPETG-motif after transpeptidation against a second recognition via Sortase-A. It is known that PEG-layers adopt different conformations (brush, mushroom) on liposomes [26]. These depend on the molar fraction of the PEGylated lipid due to interactions between adjacent polymer chains, leading to a brush-like conformation at a total PEG-densities > 4 mol% [27]. Suggesting this extended polymer conformation for DSPE-mPEG in PEG^{high}-LS, this could explain the resistance of this formulation against the reverse reaction via a steric shielding of the LPETG motif (Scheme 1) by neighboring PEG-groups.

Furthermore, polydispersity of PEG-groups in DSPE-mPEG, but not in DMA-PEG-G5 [21], may extend this shielding effect by presence of PEG-chains in DSPE-mPEG with a molecular weight larger than the 2 kDa spacer in DMA-PEG-G5. Interestingly, the PEG-layer seems to inhibit only the reverse reaction and not the recognition of the pentaglycine motif prior transpeptidation, as overall reaction efficacy of both formulations was comparable (Table 3). Compared to that, PEG^{low}-LS

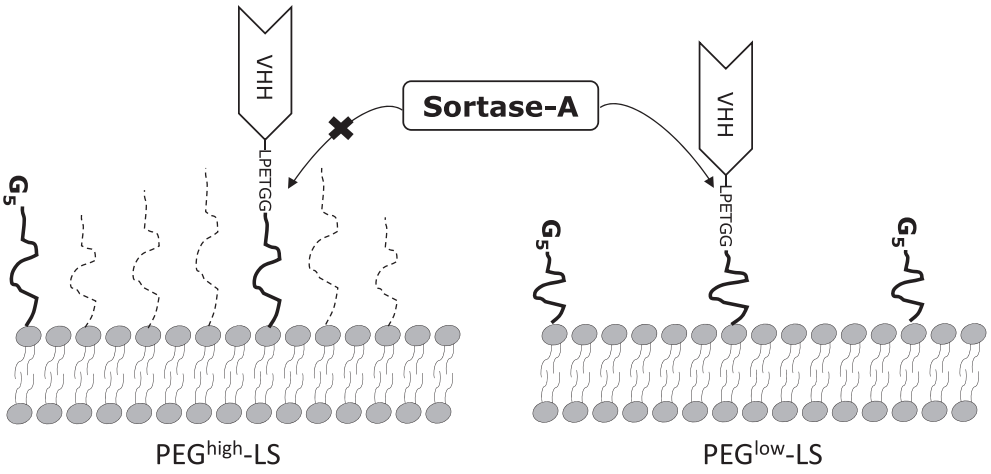

Scheme 1. Steric accessibility of LPETG-motifs on differently PEGylated bilayers. Neighboring PEG-groups in PEG^{high}-LS may shield the LPETG-motif from re-recognition by Sortase-A and therefore reduce the propensity of the reverse reaction. PEG^{low}-LS exhibit higher steric accessibility and are therefore prone for ligand cleavage by residuals of Sortase-A.

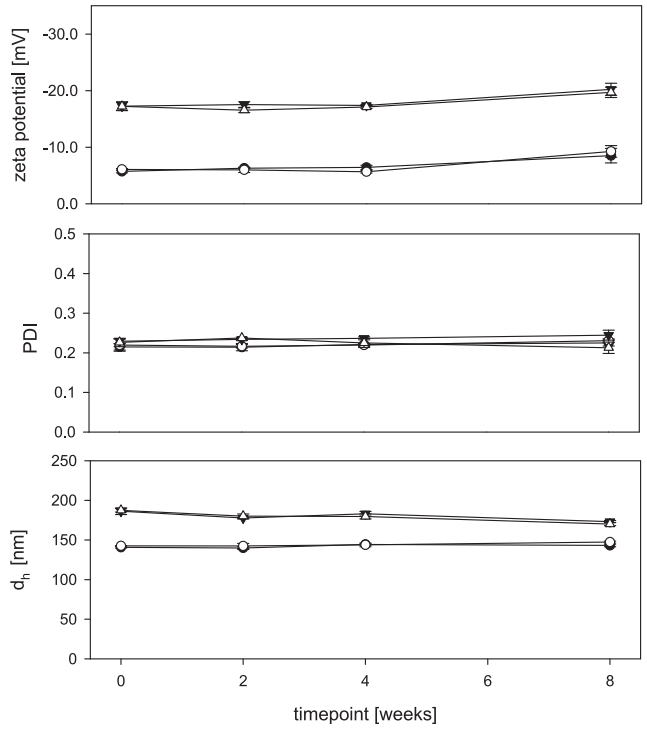

Fig. 4. Stability of VHH modified liposomes after different purification protocols. No remarkable changes in size, PDI or zeta potential occurred over an 8 weeks storage at 2–8 °C. Circles: PEG^{high}-LS; triangles: PEG^{low}-LS; black filling: dialysis; white filling: bead purification. Data shown as mean ± standard deviation of three reactions and purification procedures.

probably possess an exposed LPETG-motif in mushroom conformation due to the low (DMA-PEG-G5 derived) PEG-fraction of 1 mol%. Low interaction with neighboring polymer coils could enhance steric accessibility of the LPETG-motif between VHH and lipid anchor, leading to a pronounced reverse reaction. We furthermore tested d_h, PDI and zeta potential during storage. No relevant changes were observed over the tested time (size and PDI changes < 10%, absolute zeta potential changes < 4 mV; Fig. 4).

Sortase-A is currently gaining attraction as versatile tool to conjugate ligands on particulate drug delivery systems [5–7,9,12,18,21]. Due to the immunogenic potential of bacteria-derived protein residuals and the enzyme's inherent reversibility of the reaction, efficient purification methods are essential to ensure drug product stability and quality.

Such methods may include, especially in larger production scale, size exclusion or affinity-based chromatography. Our results indicate that especially latter frequently used method may be challenging, since considerable residuals of Sortase-A remained in the highly PEGylated formulation after affinity bead purification. Estimating a lipid dosing for the presented dialyzed PEG^{high}-LS comparable to marketed liposomal doxorubicin (Doxil®; maximum dose for the treatment of ovarian carcinoma is 50 mg doxorubicin or 400 mg total lipid per square meter of body surface), this would result in an application of 20 mg Sortase-A residuals to an average patient (1.73 m^2). The presented results therefore raise the consciousness on the drawbacks of the use of such novel conjugation techniques, which obviously put special demands on manufacturing and purification protocols. Especially the separation of Sortase or other catalytic proteins from nanoparticulate drug delivery systems can be challenging due to unspecific adsorption to the large surface of the nano-sized dispersions. Besides improvements of purification techniques, advancement of the manufacturing strategies may contribute to an avoidance of drug product instabilities by enzymatic reverse reactions. For Sortase-A, this may include the usage of primary amines (e.g. a DSPE-PEG-amine) instead of oligoglycine acceptor motifs. Primary amines are known as alternative nucleophiles during the transpeptidation [28]. As the final product would not contain a LPxTG-motif, the so obtained constructs may not be susceptible for the reverse reaction, avoiding at least stability, but not immunogenic problems. Other strategies, especially suitable for liposome modification, could involve post-insertion processes, meaning a separation of ligand lipidation and particle modification [29]. This would avoid exposure of the particulate surface with Sortase-A, thereby avoiding unspecific adsorption. Also, pre-immobilization of Sortase-A on sepharose beads could help to simplify the downstream purification of sortaggable nanoparticulate drug delivery systems [30–32].

4.2. VHH DC13-liposomes show cell type specific binding in vitro and in vivo

Liposomes functionalized with the CD11b-specific VHH DC13 or a control VHH (GFP-specific enhancer) were tested for specific binding to cells that are CD11b positive or negative. CD11b$^+$ cells included DC2.4 murine dendritic cell line [33], RAW macrophage cell line [34] and MDSC differentiated from NUP cells [24] while CD11b negative cells included undifferentiated NUP cells [24], T cells [35] and B cells [36]. Cell lines or primary splenocytes were incubated with 100 µM FITC labeled liposomes (based on total lipid content) for 4 h and analyzed by FACS and microscopy.

Untargeted PEG^{low} or PEG^{high} pentaglycine liposomes (G5-LS) and isotype control modified VHH ENH-LS did not bind to any cell type (Fig. 5A). The minor shift of the FITC signal on DC2.4 and RAW cells

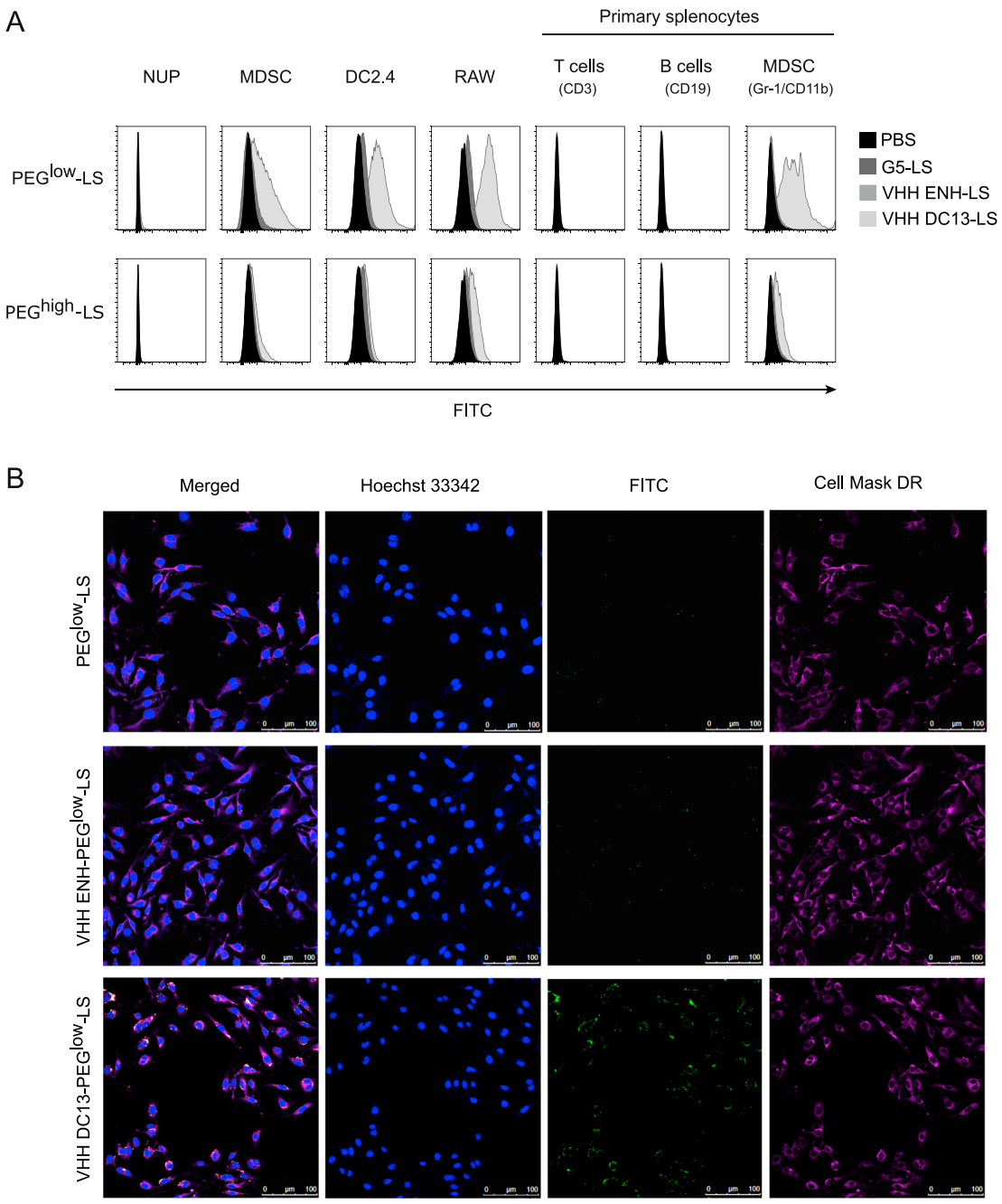

Fig. 5. In vitro binding of CD11b targeted liposomes. **A**: CD11b-positive (MDSC, DC2.4, RAW) and CD11b negative (NUP cells) cell lines were tested for the specific binding of liposomes modified with anti-CD11b VHH DC13. Furthermore, specificity of binding was investigated on isolated splenocytes including CD11b $^{+}$ MDSC and CD11b^{-} T and B cells. Both PEG^{high}- and PEG^{low}-LS bound to the cells in a ligand dependent fashion. **B**: Incubation of G5-PEG^{low}-LS, VHH ENH-PEG^{low}-LS and VHH DC13-PEG^{low}-LS with RAW macrophages. Confocal microscopy revealed cellular surface and cytosolic localization of VHH DC13-PEG^{low}-LS, but not of the control groups.

might be due to the ability of these antigen presenting cells to phagocytose small particles without any specific surface binding. Decoration with VHH DC13 induced specific surface binding on cell lines expressing CD11b (DC2.4, RAW) [33,34]. NUP cells did not show any superior interaction with the VHH DC13-modified formulations. In contrast, both VHH DC13-modified formulations were able to bind towards CD11b^{+}Gr-1^{+}MDSC differentiated from NUP cells [24].

Specificity of binding was tested using a murine splenocyte mix containing CD11b^{+}Gr-1^{+} cells, CD11b^{-}CD3^{+}T cells and CD11b^{-}CD19^{+} B cells. Parallel staining of their relevant cell surface receptors and simultaneous analysis for the liposomal FITC fluorescence revealed a specific binding towards CD11b^{+}Gr-1^{+} cells, while other cell types like T cells and B cells were unaffected (Fig. 5A).

In all cases, VHH DC13-PEG^{low}-LS showed superior binding compared to VHH DC13-PEG^{high}-LS. We demonstrated comparable VHH loading (Table 3) and antigen capturing [18] of both formulations, however, FITC-dextran encapsulation efficiency was higher for VHH DC13-PEG^{low}-LS (0.42%) than for VHH DC13-PEG^{high}-LS (0.25%). As concentrations of the dye were kept similar during solvent injection, these differences may be due to the slightly larger liposome diameter of the PEG^{low}-LS. Despite the different FITC-dextran loadings, the observed differences of in vitro binding may be due to a decreased uptake

of the PEGylated liposomes after binding. PEGylation is a widely used method to prevent uptake of the formulation by the mononuclear phagocyte system (MPS), thereby increasing in vivo circulation times [26]. In vitro, PEGylation was previously shown to reduce the uptake of liposomes by macrophages even at low molar bilayer ratios (0.5 mol%) [37]. It might therefore be that here the PEG-layer decreased uptake of the liposomes, e.g. via a PEG-induced hindrance of an effective liposome internalization. Furthermore, the additional PEG layer may reduce the steric flexibility of the conjugated VHH, and thereby decrease the cell – VHH interaction compared to the PEG^{low}-LS.

Confocal microscopy was used to investigate the specific uptake of VHH DC13-PEG^{low}-LS into RAW cells (Fig. 5B). Association with the cell surface and internalization to the cytosol was observed for VHH DC13 targeted liposomes, but not for the isotype- or uncoated control. This indicates that the sortagging of liposomes with VHH DC13 enabled the specific delivery of FITC loaded liposomes to target cells.

Although surface marker specific targeting and cellular uptake did work in vitro this may be different in vivo as the liposomes might encounter additional hurdles, such as unspecific attachment to endothelial cells, loss of target specificity, fast clearance from circulation via the MPS or blockage of the antigen-ligand interaction via plasma proteins. We injected 3 mice each intravenously with 0.6 mM of the respective VHH-conjugated liposomes (VHH ENH-LS, VHH DC13-LS, either as PEG^{low}-LS or PEG^{high}-LS) in 200 µL PBS and isolated the spleen 2 h later. The splenocytes were then stained for flow cytometry analysis to differentiate between CD11b negative T cells and B cells or CD11b$^+$Gr-1$^+$ cells. ENH-PEG^{low}-LS were used as isotype control and did not bind to any analyzed cell type (Fig. 6).

The uptake of VHH DC13-PEG^{low}-LS was increased significantly leading to a 3-fold increased FITC signal compared to VHH ENH-PEG^{low}-LS (Fig. 6B). Surprisingly this was true to the same extend for both liposomal surface types and not increased with the PEG^{low}-LS as it was the case in vitro. This might be due to different pharmacokinetic behavior of the strongly PEGylated and the anionic, charge stabilized formulation. It is known that increasing amounts of 2 kDa PEG grafting on liposomal surfaces increase the circulation time of the drug delivery system [38]. The increased circulation might therefore compensate a decreased overall binding and uptake of PEGylated formulations by the target cells. Furthermore, the presence of a broad variety of plasma proteins in vivo (which cannot be entirely simulated by the presence of FBS in vitro) may lead to enhanced alteration of lowly PEGylated surfaces due to increased unspecific protein adsorption [39]. This may lead to a decreased accessibility of the VHH on the liposomal surface and subsequently a decreased recognition of the targeted cells. These considerations indicate the need for thorough and early in vivo characterization of such targeted nanoparticulate drug delivery systems.

5. Conclusion and outlook

In the present study, Sortase-A was used to conjugate single-domain antibodies (VHHs) towards two differently PEGylated, pentaglycine modified liposomal surfaces. The resulting immunoliposomes were analyzed regarding stability against the Sortase-A inherent reverse reaction. DSPE-mPEG stabilized liposomal formulations revealed resistance against the reverse reaction, though considerable enzyme residuals were detected after a dialysis purification. DPPG stabilized PEG^{low}-LS having low PEGylation degree were prone for ligand cleavage by Sortase residuals. This could be overcome by improvement of the purification procedure and demonstrates challenges in the usage of enzyme-based conjugation methods for drug delivery system modification.

We investigated the in vitro and in vivo targeting potential of the sortagged, VHH targeted liposomes. In vitro, liposomes modified with an anti-CD11b single-domain antibody could be targeted to various CD11b$^+$ myeloid cells. This observation was successfully verified in vivo, where splenic CD11b$^+$Gr-1$^+$ cells could be targeted with clear specificity over CD11b$^-$ cells. High degree of PEGylation seemed to decrease the target cell binding in vitro. Surprisingly, this was not observed when splenic CD11b$^+$ Gr-1$^+$ cells were targeted in vivo, as both formulations performed equally. It is assumed that the extension of circulation time and reduction of unspecific plasma protein adsorption via the PEG-shell is responsible for this contrary observation. This indicates the need for an early in vivo characterization of nanoparticulate drug delivery systems, with a special regard to formulation parameters such as particle surface design.

The CD11b$^+$ and Gr-1$^+$ phenotype determines murine myeloid derived suppressors cells. This cell population exhibits the ability to suppress T cells, leading to a negative impact on the individual immune response in diseases such as cancer [20]. Thus, the here presented approach to target MDSC is attractive, e.g. for the delivery of toxins which may diminish immune suppression in the tumor microenvironment. Since CD11b is present on various other myeloid cells, a more specific targeting of MDSC may be achieved with ligands binding epitopes of Gr-1. VHHs specific for this target were recently described [19], and a combination of such ligands with nanoparticulate drug delivery systems would be a favorable option for further development. Nevertheless, CD11b$^+$ targeting might involve other promising applications such as a selective vaccine delivery [40,41] or delivery of drugs towards

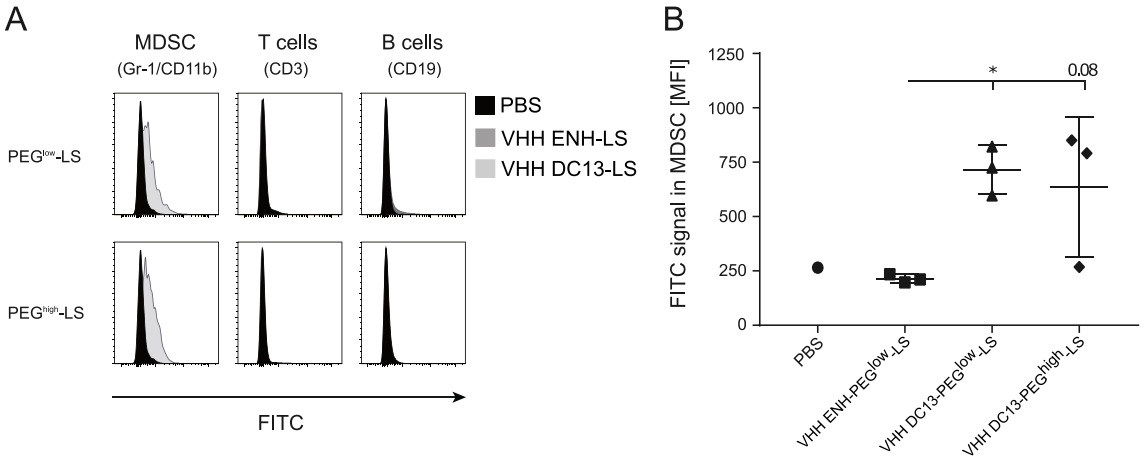

Fig. 6. In vivo targeting of splenic CD11b$^+$Gr-1$^+$ MDSC. C57BL/6J mice were injected with 0.6 mM (total lipid) of VHH DC13 modified, FITC-dextran labeled PEG^{high}-LS or PEG^{low}-LS. After 2 h incubation, mice were sacrificed and the splenocytes were analyzed for the liposomal FITC fluorescence by flow cytometry after co-staining of MDSC, T and B cell determining surface markers. **A**: Representative flow cytometry histograms. **B**: Threefold increase in MFI over the isotype control group was found for both VHH DC13 targeted formulations (significant for VHH DC13-PEG^{low}-LS ($p < 0.05$)).

atherosclerotic plaques [42].

With the presented work, manufacturing demands and formulation parameters determining the in vivo targeting of sortagged, VHH-modified liposomes were highlighted. They underline important challenges, but also the potential of such novel targeted drug delivery systems.

6. Declaration of interest

None.

References

[1] R.R. Beerli, T. Hell, A.S. Merkel, U. Grawunder, Sortase enzyme-mediated generation of site-specifically conjugated antibody drug conjugates with high in vitro and in vivo potency, PloS One 10 (7) (2015) e0131177.

[2] M. Rashidian, E.J. Keliher, A.M. Bilate, J.N. Duarte, G.R. Wojtkiewicz, J.T. Jacobsen, J. Cragnolini, L.K. Swee, G.D. Victora, R. Weissleder, H.L. Ploegh, Noninvasive imaging of immune responses, Proc. Natl. Acad. Sci. USA 112 (19) (2015) 6146–6151.

[3] J.M. Antos, G.M. Miller, G.M. Grotenbreg, H.L. Ploegh, Lipid modification of proteins through sortase-catalyzed transpeptidation, J. Am. Chem. Soc. 130 (48) (2008) 16338–16343, https://doi.org/10.1021/ja806779e.

[4] Z. Wu, X. Guo, Q. Wang, B.M. Swarts, Z. Guo, Sortase A-catalyzed transpeptidation of glycosylphosphatidylinositol derivatives for chemoenzymatic synthesis of GPI-anchored proteins, J. Am. Chem. Soc. 132 (5) (2010) 1567–1571, https://doi.org/10.1021/ja906611x.

[5] X. Guo, Z. Wu, Z. Guo, New method for site-specific modification of liposomes with proteins using sortase a-mediated transpeptidation, Bioconjugate Chem. 23 (3) (2012) 650–655.

[6] C.E. Hagemeyer, K. Alt, A.P. Johnston, Particle generation, functionalization and sortase A-mediated modification with targeting of single-chain antibodies for diagnostic and therapeutic use, Nat. Protocols 10 (1) (2015) 90–105.

[7] J.R. Silvius, R. Leventis, A novel prebinding strategy dramatically enhances sortase-mediated coupling of proteins to liposomes, Bioconjugate Chem. 28 (4) (2017) 1271–1282.

[8] H.T. Ta, S. Prabhu, E. Leitner, F. Jia, D. von Elverfeldt, K. Jackson, T. Heidt, A. Nair, H. Pearce, C. von zur Muhlen, X. Wang, K. Peter, C.E. Hagemeyer, Enzymatic single-chain antibody tagging, Circul. Res. (2011).

[9] A. Tabata, N. Anyoji, Y. Ohkubo, T. Tomoyasu, H. Nagamune, Investigation on the reaction conditions of staphylococcus aureus sortase A for creating surface-modified liposomes as a drug-delivery system tool, Anticancer Res. 34 (8) (2014) 4521–4527.

[10] S. Panowski, S. Bhakta, H. Raab, P. Polakis, J.R. Junutula, Site-specific antibody drug conjugates for cancer therapy, mAbs 6 (1) (2014) 34–45.

[11] M. Schmidt, A. Toplak, P.J.L.M. Quaedflieg, T. Nuijens, Enzyme-mediated ligation technologies for peptides and proteins, Curr. Opin. Chem. Biol. 38 (Supplement C) (2017) 1–7.

[12] M. Ritzefeld, Sortagging, A robust and efficient chemoenzymatic ligation strategy, Chem. – Eur. J. 20 (28) (2014) 8516–8529.

[13] J.M. Antos, M.C. Truttmann, H.L. Ploegh, Recent advances in sortase-catalyzed ligation methodology, Curr. Opin. Struct. Biol. 38 (2016) 111–118.

[14] U. Ilangovan, H. Ton-That, J. Iwahara, O. Schneewind, R.T. Clubb, Structure of sortase, the transpeptidase that anchors proteins to the cell wall of Staphylococcus aureus, Proc. Natl. Acad. Sci. 98 (11) (2001) 6056–6061.

[15] X. Huang, A. Aulabaugh, W. Ding, B. Kapoor, L. Alksne, K. Tabei, G. Ellestad, Kinetic mechanism of Staphylococcus aureus sortase SrtA, Biochemistry 42 (38) (2003) 11307–11315.

[16] S. Möhlmann, C. Mahlert, S. Greven, P. Scholz, A. Harrenga, In vitro sortagging of an antibody fab fragment: overcoming unproductive reactions of sortase with water and lysine side chains, ChemBioChem 12 (11) (2011) 1774–1780.

[17] W.L. Popp Maximilian, M. Antos John, L. Ploegh Hidde, Site-specific protein labeling via sortase-mediated transpeptidation, Curr. Protocols Protein Sci. 56 (1) (2009) 15.3.1-15.3.9.

[18] S. Wöll, C. Bachran, S. Schiller, M. Schröder, L. Conrad, L.K. Swee, R. Scherließ, Sortaggable liposomes: evaluation of reaction conditions for single-domain antibody conjugation by Sortase-A and targeting of CD11b+ myeloid cells, Eur. J. Pharm. Biopharm. 133 (2018) 138–158.

[19] C. Bachran, M. Schröder, L. Conrad, J.J. Cragnolini, F.G. Tafesse, L. Helming, H.L. Ploegh, L.K. Swee, The activity of myeloid cell-specific VHH immunotoxins is target-, epitope-, subset- and organ dependent, Sci. Rep. 7 (1) (2017) 17916.

[20] D.I. Gabrilovich, S. Nagaraj, Myeloid-derived suppressor cells as regulators of the immune system, Nat. Rev. Immunol. 9 (3) (2009) 162–174.

[21] S. Wöll, S. Schiller, C. Bachran, L.K. Swee, R. Scherließ, Pentaglycine lipid derivates – rp-HPLC analytics for bioorthogonal anchor molecules in targeted, multiple-composite liposomal drug delivery systems, Int. J. Pharm. 547 (1) (2018) 602–610.

[22] A. Kirchhofer, J. Helma, K. Schmidthals, C. Frauer, S. Cui, A. Karcher, M. Pellis, S. Muyldermans, C.S. Casas-Delucchi, M.C. Cardoso, Modulation of protein properties in living cells using nanobodies, Nat. Struct. Mol. Biol. 17 (1) (2010) 133–138.

[23] C. Ruedl, H.J. Khameneh, K. Karjalainen, Manipulation of immune system via immortal bone marrow stem cells, Int. Immunol. 20 (9) (2008) 1211–1218.

[24] M. Schröder, S. Loos, S.K. Naumann, C. Bachran, M. Krötschel, V. Umansky, L. Helming, L.K. Swee, Identification of inhibitors of myeloid-derived suppressor cells activity through phenotypic chemical screening, OncoImmunology 6 (1) (2017) e1258503.

[25] C. Mamot, D.C. Drummond, U. Greiser, K. Hong, D.B. Kirpotin, J.D. Marks, J.W. Park, Epidermal growth factor receptor (EGFR)-targeted immunoliposomes mediate specific and efficient drug Delivery to EGFR- and EGFRvIII-overexpressing tumor cells, Cancer Res. 63 (12) (2003) 3154.

[26] M.L. Immordino, F. Dosio, L. Cattel, Stealth liposomes: review of the basic science, rationale, and clinical applications, existing and potential, Int. J. Nanomed. 1 (3) (2006) 297–315.

[27] O. Garbuzenko, Y. Barenholz, A. Priev, Effect of grafted PEG on liposome size and on compressibility and packing of lipid bilayer, Chem. Phys. Lipids 135 (2) (2005) 117–129.

[28] J.E. Glasgow, M.L. Salit, J.R. Cochran, In vivo site-specific protein tagging with diverse amines using an engineered sortase variant, J. Am. Chem. Soc. 138 (24) (2016) 7496–7499.

[29] D.L. Iden, T.M. Allen, In vitro and in vivo comparison of immunoliposomes made by conventional coupling techniques with those made by a new post-insertion approach, Biochim. Biophys. Acta (BBA) Biomembr. 1513 (2) (2001) 207–216.

[30] M. Steinhagen, K. Zunker, K. Nordsieck, A.G. Beck-Sickinger, Large scale modification of biomolecules using immobilized sortase A from Staphylococcus aureus, Bioorg. Med. Chem. 21 (12) (2013) 3504–3510.

[31] X. Zhao, H. Hong, X. Cheng, S. Liu, T. Deng, Z. Guo, Z. Wu, One-step purification and immobilization of extracellularly expressed sortase A by magnetic particles to develop a robust and recyclable biocatalyst, Sci. Rep. 7 (1) (2017) 6561.

[32] M.D. Witte, T. Wu, C.P. Guimaraes, C.S. Theile, A.E.M. Blom, J.R. Ingram, Z. Li, L. Kundrat, S.D. Goldberg, H.L. Ploegh, Site-specific protein modification using immobilized sortase in batch and continuous-flow systems, Nat. Protocols 10 (2015) 508.

[33] M. Merad, P. Sathe, J. Helft, J. Miller, A. Mortha, The dendritic cell lineage: ontogeny and function of dendritic cells and their subsets in the steady state and the inflamed setting, Ann. Rev. Immunol. 31 (2013), https://doi.org/10.1146/annurev-immunol-020711-074950.

[34] L.J. Berghaus, J.N. Moore, D.J. Hurley, M.L. Vandenplas, B.P. Fortes, M.A. Wolfert, G.-J. Boons, Innate immune responses of primary murine macrophage-lineage cells and RAW 264.7 cells to ligands of Toll-like receptors 2, 3, and 4, Comp. Immunol., Microbiol. Infectious Diseases 33 (5) (2010) 443–454.

[35] H.I. McFarland, S.R. Nahill, J.W. Maciaszek, R.M. Welsh, CD11b (Mac-1): a marker for CD8+ cytotoxic T cell activation and memory in virus infection, J. Immunol. 149 (4) (1992) 1326.

[36] L.L. Rumfelt, Y. Zhou, B.M. Rowley, S.A. Shinton, R.R. Hardy, Lineage specification and plasticity in CD19(−) early B cell precursors, J. Exp. Med. 203 (3) (2006) 675–687.

[37] H. Xu, J.W. Paxton, Z. Wu, Enhanced pH-responsiveness, cellular trafficking, cytotoxicity and long-circulation of pegylated liposomes with post-insertion technique using gemcitabine as a model drug, Pharm. Res. 32 (7) (2015) 2428–2438.

[38] P.S. Uster, T.M. Allen, B.E. Daniel, C.J. Mendez, M.S. Newman, G.Z. Zhu, Insertion of poly(ethylene glycol) derivatized phospholipid into pre-formed liposomes results in prolonged in vivo circulation time, FEBS Lett. 386 (2) (1996) 243–246.

[39] N. Bertrand, J.-C. Leroux, The journey of a drug-carrier in the body: an anatomo-physiological perspective, J. Controlled Release 161 (2) (2012) 152–163.

[40] Y.J. Kwon, E. James, N. Shastri, J.M.J. Fréchet, In vivo targeting of dendritic cells for activation of cellular immunity using vaccine carriers based on pH-responsive microparticles, Proc. Natl. Acad. Sci. USA 102 (51) (2005) 18264–18268.

[41] J.N. Duarte, J.J. Cragnolini, L.K. Swee, A.M. Bilate, J. Bader, J.R. Ingram, A. Rashidfarrokhi, T. Fang, A. Schiepers, L. Hanke, H.L. Ploegh, Generation of immunity against pathogens via single-domain antibody-antigen constructs, J. Immunol. 197 (12) (2016) 4838.

[42] S. Katsuki, T. Matoba, S. Nakashiro, K. Sato, J.-I. Koga, K. Nakano, Y. Nakano, S. Egusa, K. Sunagawa, K. Egashira, Nanoparticle-mediated delivery of pitavastatin inhibits atherosclerotic plaque destabilization/rupture in mice by regulating the recruitment of inflammatory monocytes, Circulation 129 (8) (2013) 896–906.